This article was downloaded by:
On: *29 January 2011*
Access details: *Access Details: Free Access*
Publisher *Taylor & Francis*
Informa Ltd Registered in England and Wales Registered Number: 1072954 Registered office: Mortimer House, 37-41 Mortimer Street, London W1T 3JH, UK

Supramolecular Chemistry
Publication details, including instructions for authors and subscription information:
http://www.informaworld.com/smpp/title~content=t713649759

Metal Complexes of an Oxatriaza Macrocycle Containing Pyridine: Thermodynamic Stability and Structural Studies

Judite Costa[ab]; Rita Delgado[ac]; Maria Teresa Duarte[cd]; Vítor Félix[ae]
[a] Instituto de Tecnologia Química e Biológica, Oeiras, Portugal [b] Faculdade de Farmácia de Lisboa, Lisboa, Portugal [c] Instituto Superior Técnico, Lisboa, Portugal [d] Centro de Química Estrutural, Lisboa, Portugal [e] Dep. Química, Universidade de Aveiro, Aveiro, Portugal

To cite this Article Costa, Judite , Delgado, Rita , Duarte, Maria Teresa and Félix, Vítor(2001) 'Metal Complexes of an Oxatriaza Macrocycle Containing Pyridine: Thermodynamic Stability and Structural Studies', Supramolecular Chemistry, 13: 2, 333 — 347
To link to this Article: DOI: 10.1080/10610270108027488
URL: http://dx.doi.org/10.1080/10610270108027488

PLEASE SCROLL DOWN FOR ARTICLE

Full terms and conditions of use: http://www.informaworld.com/terms-and-conditions-of-access.pdf

This article may be used for research, teaching and private study purposes. Any substantial or systematic reproduction, re-distribution, re-selling, loan or sub-licensing, systematic supply or distribution in any form to anyone is expressly forbidden.

The publisher does not give any warranty express or implied or make any representation that the contents will be complete or accurate or up to date. The accuracy of any instructions, formulae and drug doses should be independently verified with primary sources. The publisher shall not be liable for any loss, actions, claims, proceedings, demand or costs or damages whatsoever or howsoever caused arising directly or indirectly in connection with or arising out of the use of this material.

SUPRAMOLECULAR CHEMISTRY, Vol. 13, pp. 333–347
Reprints available directly from the publisher
Photocopying permitted by license only

© 2001 OPA (Overseas Publishers Association) N.V.
Published by license under
the Gordon and Breach Science
Publishers imprint.

Downloaded At: 15:31 29 January 2011

Metal Complexes of an Oxatriaza Macrocycle Containing Pyridine: Thermodynamic Stability and Structural Studies

JUDITE COSTA[a,b], RITA DELGADO[a,c,*], MARIA TERESA DUARTE[c,d] and VÍTOR FÉLIX[a,e]

[a]*Instituto de Tecnologia Química e Biológica, UNL, Apartado 127, 2781-901 Oeiras, Portugal;* [b]*Faculdade de Farmácia de Lisboa, Av. das Forças Armadas, 1600 Lisboa, Portugal;* [c]*Instituto Superior Técnico, Av. Rovisco Pais, 1049-001 Lisboa, Portugal;* [d]*Centro de Química Estrutural, Av. Rovisco Pais, 1049-001 Lisboa, Portugal;* [e]*Dep. Química, Universidade de Aveiro, Campus de Santiago, 3810-193 Aveiro, Portugal*

(Received 16 May 2000)

A new 14-membered oxatriaza macrocycle containing pyridine has been synthesized, 7-oxa-3,11,17-triazabicyclo[11.3.1]heptadeca-1(17),13,15-triene, L^1. The protonation constants of this compound and stability constants of its complexes with the Mn^{2+} to Zn^{2+}, Cd^{2+}, and Pb^{2+} were determined by potentiometric methods at 25°C and ionic strength 0.10 mol dm^{-3} in KNO_3. L^1 presents two high values of protonation constants, and the third is very low. Its overall basicity is low because the three basic centres are in close proximity. Only mononuclear complexes were found, and the stability constants with all the metal ions studied are of the same order as those of the corresponding complexes of the oxatriaza macrocycle L^2 (1-oxa-4,8,12-triazacyclotetradecane), but lower than those of tetraaza macrocycles of similar or lower cavity size. The electronic spectra together with the values of magnetic moments of the cobalt(II) and nickel(II) complexes of L^1 suggest that five co-ordinate species are formed in aqueous solution. The EPR spectroscopy of frozen solutions of the copper(II) complex of L^1 has shown only one species characteristic of rhombic symmetry with elongation of the axial bonds and a $d_{x^2-y^2}$ ground state, and the analysis of the EPR parameters suggests the presence of a bis complex containing two macrocyclic units. The single crystal structure of the complex $[CuL^1Cl]ClO_4$ 1 was determined. The complex crystallises in the triclinic system, space group $P\bar{1}$, $a = 7.4973(9)$, $b = 9.649(2)$, $c = 12.712(2)$ Å, $\beta = 111.02(2)$, $\beta = 96.65(1)$, $\gamma = 90.11(1)°$, $Z = 2$, $D_{calcd} = 1.691\,g\,cm^{-3}$. Final R and R' values of 0.0578 and 0.1454 for 2603 reflections with $I > 2\sigma(I)$ and 0.0782 and 0.1619 for all data were obtained. The complex displays a distorted square pyramidal co-ordination sphere, the three nitrogen atoms of the macrocycle and one chlorine atom determining the basal plane and the apical position occupied by the oxygen atom of the macrocyle. The metal centre is 0.275(2) Å away from the N_3Cl plane towards to the apical ligand giving rise to a Cu–O bond length of 2.247(4) Å. To achieve this geometric arrangement the oxatriaza macrocycle folds about the line defined by the nitrogen atoms contiguous to the pyridine ring leading to a dihedral angle of 72.2(2)°. The single crystal presents a 1-*D* centrosymmetric supramolecular structure formed by two chains of cations and anions linked by hydrogen bonding *via* N–H···O and $C-H^{\delta+}\cdots O^{\delta-}$ intermolecular interactions.

Keywords: Oxatriazamacrocycles; Stability constants; Single crystal X-ray structure; Hydrogen-bonding interactions; EPR spectroscopy of copper(II) complex; Molecular aggregates

*Corresponding author. e-mail: delgado@itqb.unl.pt

Downloaded At: 15:31 29 January 2011

INTRODUCTION

Comparative studies of the behaviour of metal complexes of 12- to 14-membered tetraaza and oxatriaza macrocycles, as well as of their acid-base reactions, have been carried out [1,2]. In spite of the substantial number of data collected and analysed, namely, thermodynamic [1] and structural [2] data, some doubts persisted about the interpretation of the steep fall of stability constant values of the complexes of the 14-membered oxatriaza macrocycles in relation to those of the tetraaza macrocycle of the same cavity size. However, the 14-membered macrocycles of these two series in comparison were not structurally equivalent, due to synthetic difficulties [1], and it is well known that small differences in the macrocyclic backbone can induce significant differences in the behaviour of the metal complexes [3,4]. Indeed, in the 14-membered oxatriaza macrocycle (L^2) the two six- and two five-membered chelate rings are in consecutive positions, while the tetraaza macrocycle, *cyclam* (1,4,8,11-tetraazacyclotetradecane), alternate five- and six-membered chelate rings exists. Another study of the effect of the replacement of a nitrogen by an oxygen donor atom in the ring was undertaken for smaller macrocycles, namely 9- and 10-membered triaza and oxadiaza macrocycles, but in this case the small cavity size of the macrocycles and the propensity to form ML_2 complexes does not allow general conclusions [5].

In the present work we have prepared the 14-membered oxatriaza macrocycle L^1, which is structurally equivalent to the tetraaza macrocycle L^3 already studied [6,7], and the objective of the work is to compare the behaviour of both ligands and their complexes. The study will be extended to the 14-membered oxatriaza macrocycle (L^2) which does not contain pyridine for comparison purposes.

All macrocyclic compounds mentioned along the text are presented in Scheme 1.

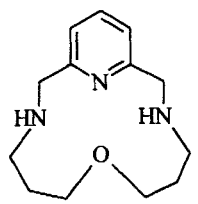

L^1

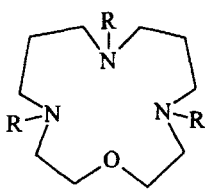

L^2 - R = R' = H
L^{12} - R = R' = CH_3

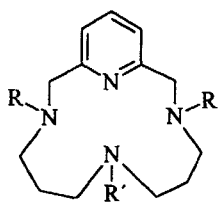

L^3 - R = R' = H
L^6 - R = H; R' = CH_3
L^7 - R = R' = CH_3
L^8 - R = R' = 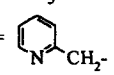
L^9 - R = $(\eta^5\text{-}C_5H_5)_2Fe\text{-}CH_2$- ; R' = CH_3

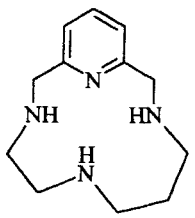

L^4

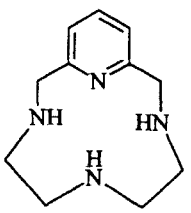

L^5

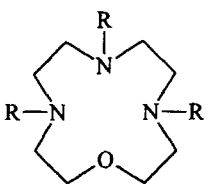

L^{10} - R = R' = H
L^{11} - R = R' = CH_3

SCHEME 1

RESULTS AND DISCUSSION

Synthesis of the Macrocycle

The compound L^1 has been synthesized by a template reaction using a procedure similar to that already used for L^3 [6]. The worse yield obtained in the former case is probably related with the lower stability of the copper(II) complex formed during the cyclization reaction, due to the presence of oxygen atom, and to the adopted geometry which prevents the achievement of the square planar arrangement of the donor atoms necessary for a good yield [8]. In spite of this we selected the template reaction for the preparation of L^1 because it is less time consuming than all the other possible procedures.

Protonation Reactions

The oxatriaza macrocycle L^1 has two high values of protonation constants, as expected by comparison with similar macrocyclic ligands such as those listed in Table I, which correspond to the protonation of the two secondary amines. These two constants are only slightly lower than the corresponding values of the 14-membered oxatriaza and tetraaza macrocycles, L^2 and L^3, respectively, and very similar to those of the 13-membered tetraaza macrocycle, L^4. However, the second protonation constant of the 12-membered tetraaza macrocycle, L^5, is lower [6]. These facts indicate that the two first protonation constants are weakly affected by the greater inductive effect of the ether oxygen in close

Downloaded At: 15:31 29 January 2011

TABLE I Protonation (log K_i^H) constants of L^1-L^5, and stability constants (log $K_{M_mH_hL_l}$) of their complexes with several divalent metal ions. $T = 25.0°C$; $I = 0.10$ mol dm^{-3} in KNO_3

Ion	Equilibrium Quotient	$L^{1(a)}$	$L^{2(b)}$	$L^{3(c)}$	$L^{4(c)}$	$L^{5(c)}$
H^+	[HL]/[L] × [H]	9.27(2)	10.097	9.92	9.79	10.33
	[H_2L]/[HL] × [H]	8.49(3)	8.673	8.56	8.49	7.83
	[H_3L]/[H_2L] × [H]	< 2	4.65	4.66	2.85	1.27
	[H_3L]/[L] × [H]^3	< 19.8	23.42	23.14	21.13	19.43
Mn^{2+}	[ML]/[M] × [L]	3.61(3)	–	5.477	7.29	8.81
	[ML]/[MLOH] × [H]	–	–	–	9.93	–
Co^{2+}	[ML]/[M] × [L]	7.15(1)	8.87	–	–	–
	[MHL]/[ML] × [H]	–	5.73	–	–	–
	[ML]/[MLOH] × [H]	10.02(8)	–	–	–	–
Ni^{2+}	[ML]/[M] × [L]	9.83(1)	9.7	16.267	16.81	17.05
	[MHL]/[ML] × [H]	–	7.0	–	–	–
	[ML]/[MLOH] × [H]	10.62(4)	–	–	–	–
Cu^{2+}	[ML]/[M] × [L]	15.54(1)	15.4	19.76	18.62	20.14
	[MHL]/[ML] × [H]	–	6.0	–	–	–
	[ML]/[MLOH] × [H]	7.24(3)	–	–	10.4	7.48
Zn^{2+}	[ML]/[M] × [L]	6.86(2)	8.9	12.816	14.27	14.40
	[MHL]/[ML] × [H]	–	7.1	–	–	–
	[ML]/[MLOH] × [H]	–	–	8.48	7.83	8.5
Cd^{2+}	[ML]/[M] × [L]	6.35(1)	7.13	9.759	11.64	12.670
	[ML]/[MLOH] × [H]	9.73(6)	9.19	10.30	10.02	10.44
Pb^{2+}	[ML]/[M] × [L]	6.74(2)	7.30	9.715	12.275	15.422
	[ML]/[MLOH] × [H]	9.03(3)	8.9	10.948	9.99	10.58

(a) Values in parenthesis are standard deviations in the last significant figures.
(b) Ref. [1].
(c) Ref. [6].

proximity and more influenced by the size of the macrocycle.

The third protonation constant is very low and cannot be obtained by potentiometric measurements. This constant corresponds to the protonation of the pyridine nitrogen in close proximity to the other two protonated nitrogen and the strong repulsion between charges turns this nitrogen very acidic. Compound L^5 also exhibits a very low log K_3 for identical reasons, although in this case the sequence of protonation is completely different, as a ^1H NMR spectroscopy titration has revealed [6]. The basicity increases with increase of the distance of the third basic centre from the other two already protonated and so with the cavity size of the macrocycle, being log K_3 larger for L^4, and much larger for L^3 or L^2.

In conclusion the overall basicity of L^1 is of the order of that of L^5 but smaller than that of the other two 14-membered macrocycles, L^2 and L^3.

Complexation Reactions

Stability Constants

The stability constants of L^1 with most of the first transition metal ions, Cd^{2+} and Pb^{2+} are collected in Table I together with the constants of the complexes of L^2–L^5 for comparison [1,6]. Only mononuclear complexes were found. We have checked the possibility of formation of the bis complex $M(L^1)_2$, but it is not formed in aqueous solution under our conditions. Indeed this species is chemically expected because the macrocycle has enough flexibility to achieve a folded conformation with three donor atoms in the right position (three nitrogen or two nitrogen and one oxygen atoms) to encapsulate the metal centre in facial fashion, two macrocyclic units leading to hexaco-ordinated species (see below).

The values of stability constants of L^1 with all the metal ions studied are of the same order of those of the corresponding complexes of the oxatriaza macrocycle L^2, but lower than those of the tetraaza macrocycles, L^3–L^5, (*cf.* Tab. I). The differences of the log stability constants of complexes of the same metal of L^1 and L^2 are smaller than expected if only the overall basicity of both ligands was taken into account, the stability of the former complexes being comparatively higher.

On the other hand, the differences between the stability constants (log values) of the metal complexes of L^1 and those of the tetraaza macrocycle L^3 are smaller for the Mn^{2+} and Pb^{2+} complexes, and larger for the Ni^{2+} to Zn^{2+} ones. The Cd^{2+} complexes show an intermediate behaviour. These differences ($\log K_{ML} - \log K^1_{ML}$, L being the ligand to be compared) increase systematically with the decrease of the cavity size of the macrocycle for the complexes of the larger metal ions: for the Pb^{2+} complexes they are 2.98, 5.36 and 8.68, and for the Mn^{2+} complexes, 1.87, 3.68 and 5.20 when L is L^3, L^4 and L^5, respectively. However, while ($\log K_{ML} - \log K^1_{ML}$) are large for the Ni^{2+} to Zn^{2+} complexes when $L = L^3$, these differences increase only slightly with the decrease of the cavity size of L. In fact, on one hand, the last metal ions, forming mainly covalent bonding interactions on complexation, prefer ligands containing nitrogen atoms, while the presence of the oxygen donor stabilises complexes of Mn^{2+} or Pb^{2+}. On the other hand, it is well known that the 12-membered macrocycles stabilise better metal ions of larger ionic sizes, while the 14-membered ones prefer the complexation of smaller metal ions, such as Ni^{2+} or Cu^{2+}. The reason for this apparent paradox comes from the fact that the complexes of the 12-membered macrocycles adopt folded conformations, or planar ones with the metal ion necessarily above the donor atoms plane, but cannot encapsulate metal ions in planar conformations. In contrast, the 14-membered macrocycles can adopt planar conformations in complexes of small metal ions, such as Co^{2+} to Zn^{2+}, because their cavity sizes can easily accommodate them [4,7,9,10].

Downloaded At: 15:31 29 January 2011

Downloaded At: 15:31 29 January 2011

Spectroscopic Studies

The cobalt(II) complex of L^1 exhibits an electronic spectrum with several small bands in the infrared region, another one at 778 nm, and a multiply structured visible band, see Table II. This electronic spectrum and the intensity of the bands together with the magnetic moment of 4.54 μ_B point to a five co-ordinate environment [11,12]. Bertini *et al.*, suggest that when the spectrum shows a weak absorption between 830 and 670 nm, as it is the case in our complex, a five co-ordinated species is present [11].

The electronic spectrum of the nickel(II) complex of L^1 exhibits five broad but well defined bands and several shoulders (*cf.* Tab. II), characteristic of five co-ordinate high-spin complexes [12–17]. The magnetic moment of 3.40 μ_B also falls in the range normally observed for high-spin five co-ordinate Ni^{2+} chromophores [12,13,18]. However, without X-ray diffraction analysis the stereochemical arrangement of five co-ordinate nickel(II) is not safely assigned. The non-equivalence of the donor atoms of the ligand also contributes to the difficulty in assignment of a strictly trigonal bipyramidal or a square pyramidal geometry, and probably an intermediate structure is what actually occurs.

The Cu^{2+} complex exhibits a broad band in the visible region at 601 nm with one shoulder at lower energies due to the copper d–d transitions, an intense band in the UV region and a broad band in the near-IR region. The EPR spectra of the complex were performed at a large pH range, 3.80 to 6.10. They are all similar and show the presence of only one species, in agreement with the potentiometric results, see Figure 1. The spectra exhibit the four expected lines at low field and no superhyperfine splitting has been observed. The simulation of the spectra [19] indicated three different principal values of g, revealing that the Cu^{2+} ion in this complex is in a rhombically-distorted ligand field. In Table III are compiled the hyperfine coupling constants (A) and g values, which are characteristic of rhombic symmetry with elongation of the axial bonds and $d_{x^2-y^2}$ ground state. Elongated

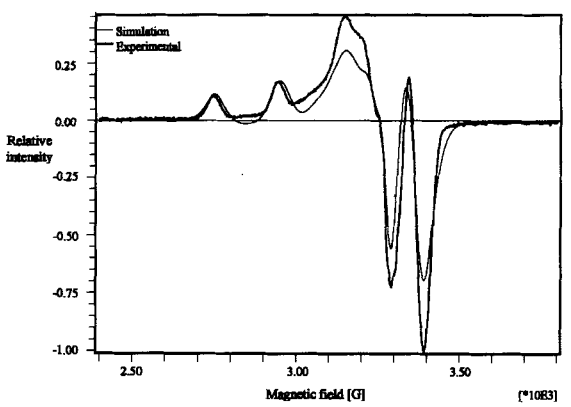

FIGURE 1 EPR X-band spectrum of the Cu^{2+} complexes of L^1 recorded at 127 K, microwave power of 2.4 mW, modulation amplitude of 1.0 mT. The frequency (ν) was of 9.41 GHz.

TABLE II Spectroscopic UV-*vis*-near IR data and magnetic moments for the Co^{2+}, Ni^{2+}, and Cu^{2+} complexes of L^1 (T = 25.0°C)

Complex Colour	pH	UV-vis-nearIR λ_{max}/nm(ε_{molar}/dm^{3}mol^{-1}cm^{-1})	μ/μ_B
$[CoL^1X]^+$ (orange)	7.10	1051 (6.9), 991 (sh, 6.3), 778 (sh, 19.4), 708(sh, 8.0), 641 (17.7), 476 (sh, 47.6), 461 (87.5); 282 (sh, 1636); 270 (sh, 3860); 264 (4474)	4.54
$[NiL^1X]^+$ (yellow)	7.99	1159 (26.5), 904 (sh, 52.6), 860 (sh, 62), 783 (84.4), 734 (91), 680 (83.3), 530 (105.2); 270(sh, 3064); 266 (3513); 262 (3977)	3.40
$[CuL^1X]^+$ (blue)	5.66	1160 (6.3), 913 (9.7), 691 (sh, 74.3), 601 (158.3), 280 (sh, 3139), 270 (sh, 5391), 264 (sh, 7435), 256 (3917)	–

TABLE III Spectroscopic EPR data for the Cu^{2+} complexes of L^1 and other similar complexes

Copper(II) Complex	Visible band nm (ε_{molar}/ $dm^3mol^{-1}cm^{-1}$)	EPR $A_i \times 10^4 cm^{-1}$ g_x	g_y	g_z	A_x	A_y	A_z	Point (in Fig. 2)	Ref.
$[CuL^1Cl]^+$	601 (158.3)	2.050	2.097	2.199	6.4	41.1	208.9	**12**	[a]
$[CuL^3]^{2+}$	560 (187)	2.034	2.060	2.188	0.5	3.4	192.9	**11**	6, 24
$[CuL^4Br]^+$	580 (192)	2.040	2.052	2.188	23.8	43.1	197.7	**10**	6
$[CuL^5Br]^+$	695 (161)	2.033	2.084	2.210	26.6	38.9	161.0	**9**	6
$[CuL^2(H_2O)]^{2+}$	622 (147)	2.050	2.059	2.224	10.9	20.5	183.1	**4**	2
$[CuL^{12}(Cl)]^+$	680 (262)	2.053	2.058	2.224	10.5	24.3	183.4	**5**	2
$[CuL^{13}(N_3O)]^+$	626.4 (160)	2.027	2.082	2.216	26.9	15.1	160.2	**3**	2
$[CuL^{10}(Br)]^+$	690.6 (161)	2.037	2.077	2.226	23.8	21.6	162.8	**1**	2
$[CuL^{11}(Cl)]^+$	675 (340)	2.051	2.081	2.228	27.5	10.4	157.2	**2**	2
[Cu(*cyclam*)(NO_3)]$^+$	513 (100)	2.049		2.186		38.7	205.0	**8**	26
[Cu(*cyclen*)(NO_3)]$^+$	599 (220)	2.057		2.198		24.1	184.2	**7**	26
[Cu(*cyclen*)(Cl)]$^+$	594 (271)	2.089		2.172		31	177.5	**6**	25
$[Cu([9]aneN_3)_2]^{2+}$	614	2.055		2.229		22	177	**13**	28
$[Cu([9]aneN_2O)_2]^{2+}$	546	≈2.04		2.205		27	198	**14**	27

[a] This work.

Downloaded At: 15:31 29 January 2011

rhombic-octahedral, rhombic square-coplanar or distorted square pyramidal stereochemistries are consistent with these data, but trigonal-bipyramidal or tetragonal geometries involving compression of axial bonds can be excluded [10, 17, 20, 21].

According to the ligand field theory, the g_z values increase and the A_z values decrease as the equatorial ligand field becomes weaker or as the axial ligand field becomes stronger, and this occurs with the simultaneous red-shift of the d – d absorption bands in the electronic spectra [10, 17, 22, 23]. However, this is not verified for the case of the copper(II) complex of L^1. In Figure 2 is shown a diagram of A_z *versus* g_z for several 12- to 14-membered tetraaza and oxatriaza macrocycles, all of them performed in the same experimental conditions and published before by us [2, 6, 24], and others [25, 26], and the parameters are collected in Table III. The bis complexes of two 9-membered macrocycles have also been added, $[Cu([9]aneN_2O)_2]^{2+}$ [27] and $[Cu([9]aneN_3)_2]^{2+}$ [28], where [9]aneN_2O and [9]aneN_3 are 1-oxa-4,7-diazacyclononane and 1,4,7-triazacyclononane, respectively.

As expected, the complexes of tetraaza macrocycles, containing or not pyridine, are located on

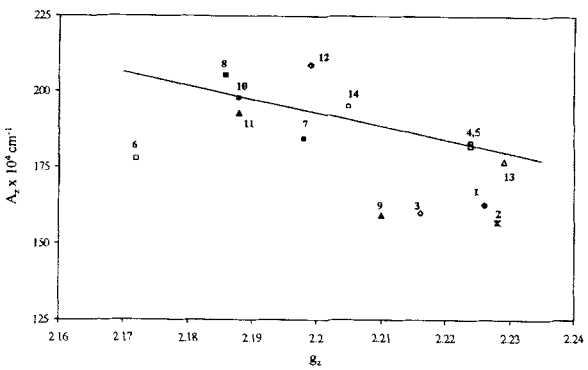

FIGURE 2 Diagram of the EPR parameters A_z *versus* g_z for a series of copper(II) complexes of tetraaza and oxatriaza macrocycles, namely: **1** – L^{10}; **2** – L^{11}; **3** – L^{13}; **4** – L^2; **5** – L^{12}; **6** – *cyclen* with Cl^- as fifth donor atom; **7** – *cyclen* with NO_3^- as fifth donor atom; **8** – *cyclam*; **9** – L^5; **10** – L^4; **11** – L^3; **12** – L^1. Compound L^{13} is 1-oxa-4,7,11-triazacyclotridecane and **13** and **14** are respectively the values of the sandwich copper(II) complexes of the 1,4,7-triazacyclononane and 1-oxa-4,7-dizacyclononane.

the left part of the diagram, with higher A_z and lower g_z parameters, and the oxatriaza macrocycles are located on the right part, with lower A_z and higher g_z values, because nitrogen atoms are more electron-rich than oxygen ones. The line is the mean least-squares straight line of the points corresponding to the EPR parameters of copper(II) complexes which exhibit square-

Downloaded At: 15:31 29 January 2011

planar (point **11**) or square-pyramidal geometry where the donor atoms of the macrocycle form the equatorial plane and a monodentade ligand occupies the apical position (points **4,5,8,10**). Below this line are the points corresponding to pentaco-ordinate complexes adopting square pyramidal or trigonal pyramidal geometries in which the macrocycle is folded and the monodentade ligand is in equatorial position. The EPR parameters obtained for all complexes in frozen solutions could be explained on the basis of their X-ray diffraction structures, even if in certain cases some difficulties of interpretation arised, as in the cases of points **6** and **3** of the diagram [2, 6]. The pentaco-ordinate complexes where the macrocycles adopt folded conformations have lower A_z and higher g_z values as predicted by the ligand field theory. However, two copper(II) complexes present very exceptional behaviour, A_z being very high and g_z very low for N_3O and N_4O_2 co-ordination spheres, as happens with our complex, point **12** and the bis complex $[Cu([9]aneN_2O)_2]^{2+}$ (point **14**). We also do not have an explanation for the position of the other bis complex, $[Cu([9]aneN_3)_2]^{2+}$, point **13**, which has lower A_z and higher g_z values than expected. The EPR spectrum of the complex in study in this work was first performed in the presence of nitrate anion, and some months later in the presence of chloride, exhibiting always the same parameters. Its crystal structure has revealed that the macrocycle is folded and that the oxygen of the macrocyclic backbone occupies the apical position (see below), a structure which is comparable to those adopted by the copper(II) complexes of L^{10} and L^{11} [2] (points **1** and **2**, respectively), and so similar EPR parameters should be expected for the three complexes. Surprisingly, the EPR parameters of the copper(II) complex of L^1 are similar to those of the sandwich complex $[Cu([9]aneN_2O)_2]^{2+}$ (point **14**), suggesting that in our case a bis complex containing two macrocyclic units should also be formed in frozen solution.

X-ray Single Crystal Diffraction

The structure of the complex $[CuL^1Cl](ClO_4)$ **1** was determined by single crystal X-ray diffraction. Complex **1** is built up of an asymmetric cell consisting of one cationic complex $[CuL^1Cl]^+$ and one ClO_4^- anion. An ORTEP view of the complex cation $[CuL^1Cl]^+$ **1** showing the molecular geometry and the atomic labelling scheme adopted is presented in Figure 3. For simplicity reasons the complex and the corresponding cation have the same number. Bond lengths and angles centred at the copper(II), listed in the Table IV, indicate that the complex has a distorted square pyramidal co-ordination

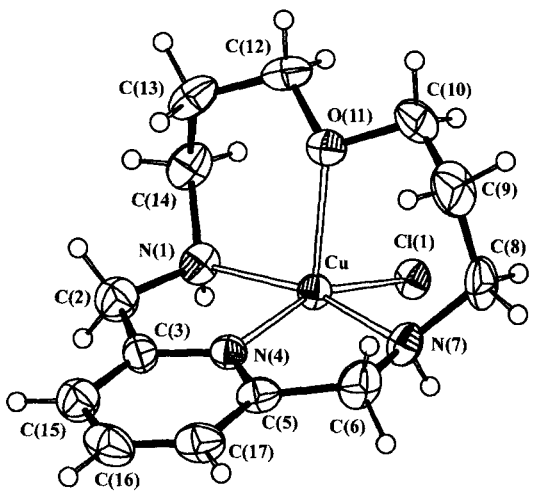

FIGURE 3 An ORTEP view of $[CuL^1Cl]^+$ **1** showing the molecular geometry and the labelling scheme adopted. Thermal ellipsoids are drawn at 40% of probability level.

TABLE IV Selected bond lengths (Å) and angles (°) in the copper(II) co-ordination sphere of the cation complex $[CuL^1Cl]^+$ **1**

Lengths			
Cu–O(11)	2.247(4)		
Cu–N(1)	2.034(5)	Cu–N(4)	1.938(5)
Cu–N(7)	2.036(5)	Cu–Cl(1)	2.280(1)
Angles			
N(4)–Cu–O(11)	103.8(2)	N(1)–Cu–O(11)	94.7(2)
N(7)–Cu–O(11)	92.5(2)	O(11)–Cu–Cl(1)	99.8(1)
N(1)–Cu–Cl(1)	96.5(2)	N(7)–Cu–Cl(1)	96.6(2)
N(1)–Cu–N(7)	163.8(2)	N(4)–Cu–Cl(1)	156.5(1)
N(4)–Cu–N(1)	82.2(2)	N(4)–Cu–N(7)	81.9(2)

Downloaded At: 15:31 29 January 2011

sphere. Three nitrogen atoms of L^1 and one chlorine atom determine the basal plane. This plane exhibits a tetrahedral distortion relative to the mean least-squares plane determined by the atoms N(1), N(4), N(7) and Cl(1). The deviations from the mean square plane are −0.150(2) Å for N(1) and N(7), +0.182(3) Å for N(4) and +0.118(2) Å for Cl(1). The apical co-ordination is accomplished *via* the oxygen atom of the macrocyclic backbone, which is at a distance of 2.521(5) Å from that plane. The metal centre is 0.275(2) Å away from the N_3Cl plane towards to the apical atom giving rise to a Cu–O bond length of 2.247(4) Å. Furthermore the Cu–O bond is almost perpendicular to the N_3Cl equatorial co-ordination plane giving an angle between the Cu–O vector and this plane of 88.9(1)°. To achieve this geometric arrangement the oxatriaza macrocycle folds remarkably about the line defined by the nitrogen atoms N(7) and N(1) leading to a dihedral angle between the planes formed by the atoms N(1),N(4),N(7) and N(1),O(11),N(7) of 72.2(2)°.

The macrocycle in complex **1** adopts the folded conformation **+−+e**, in which the two H-N groups and the electron lone pair of the oxygen atom are located in opposite sides of the N_3O macrocyclic plane. Furthermore in this conformation the Cl and the two N–H groups are on the same side of the macrocyclic plane. The + and − signs indicate that the N-substituent groups are located above or below the macrocyle plane, respectively, and the label **e** indicates that the Cl occupies an equatorial position of the square pyramidal geometric arrangement. This nomenclature was used in the study undertaken for L^3 and its N-derivatives [7], and was adapted for the case of oxatriaza macrocycles by replacing one N-substituent group by the location of the lone electron pair of the oxygen atom.

A comparable geometric arrangement to that described for the studied complex was found for the five co-ordinated complex $[CuL^8]^{2+}$ **2**, being L^8 the N-tris(2-pyridylmethyl) derivative of L^3 [29]. This macrocycle shows also a pronounced folding of 76.5(3)° about the axis defined by the two nitrogen atoms contiguous to the pyridine ring of the macrocycle, and the apical position is occupied by the nitrogen atom *trans* to this pyridine ring. The fifth co-ordination position on the equatorial plane is occupied by one nitrogen atom from a pyridylmethyl pendant arm. The two remaining pyridylmethyl arms stay uncoordinated.

As expected the Cu–N(sp^2) distance of 1.938(5) Å in **1** is shorter than the two Cu–N(sp^3) distances, for which the average value is 2.035(5) Å. A similar pattern of Cu–N distances with slightly longer values were found for complex **2**, in which the Cu–N(sp^2) and the average Cu–N(sp^3) distances involving the two nitrogen atoms contiguous to the pyridine ring are 1.962(7) and 2.064(8) Å, respectively. Moreover the related five co-ordinated complexes $[CuL^6(NO_3)]^+$ **3** [30], $[CuL^9Cl]^+$ **4** [31], and $[CuL^9I]^+$ **5** [31], which have the respective monodentate ligands in apical position, exhibit Cu–N(sp^2) and Cu–N(sp^3) distances comparable to those reported for the studied complex, which are respectively 1.934(2) and 2.027(2) Å in **3**, 1.921(2) and 2.096(10) Å in **4**, and 1.928(7) and 2.095(2) Å in **5**.

The Cu–O apical distance of 2.247(4) Å in **1** is longer than the equatorial Cu–N distances due basically to the Jahn-Teller effect and not to either steric strain imposed by a poor match between the cavity of the macrocycle in the **+−+e** conformation and the size of the metal ion. The complex $[CuL^8]^{2+}$ **2** [29] has also an apical Cu–N(sp^3) distance [2.198(8) Å] longer than the equatorial ones [average value 2.064(8) Å]. The lower difference is obviously due to the smaller size of the nitrogen atom compared to the oxygen. In contrast, in the zinc square pyramidal complex $[ZnL^9Cl]^+$ **6** [31], in spite of the larger ion size of the Zn^{2+} compared to Cu^{2+}, the macrocycle also adopts a **+−+e** conformation, where this electronic effect is absent, but the apical Zn–N distance of

2.066(20) Å is strikingly shorter than the equatorial ones of 2.177(17) and 2.228(17) Å. This pattern of distances was ascribed to the presence of the two appended bulky ferrocenyl groups on the nitrogen of the macrocycle instead of any steric strain caused by the +−+e arrangement of L^9 [31]. Additionally, the Cu−O apical distance in **1** is comparable to that found in the square pyramidal complexes $[CuL^{10}Br]^+$ **7** [2] and $[CuL^{11}Cl]^+$ **8** [2] in which the oxygen donor atom of the 12-membered oxatriaza macrocycles is also in an apical position [2.347(7) and 2.216(6) Å, respectively]. On the other hand, the five-coordinated copper(II) complexes of

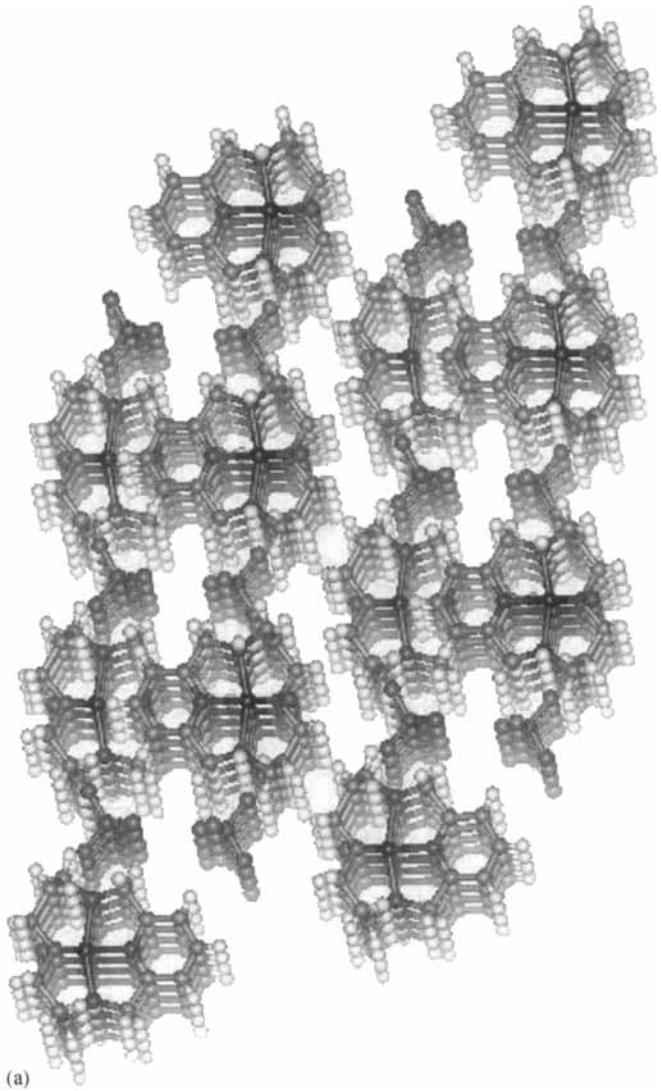

FIGURE 4 Crystal packing of the complex $[CuL^1Cl](ClO_4)$ **1**. (a) View along the *a* crystallographic axis showing how the packing of chains cations, related by inversion centre, results in the π-stacking of pyridine rings. (b) View down the *b* crystallographic axis showing the centrosymmetric supramolecular structure derived from the interactions of two one-dimensional chains of cations and anions *via* hydrogen bonds. For clarity the hydrogen atoms were omitted, apart those involved in hydrogen bonding.

Downloaded At: 15:31 29 January 2011

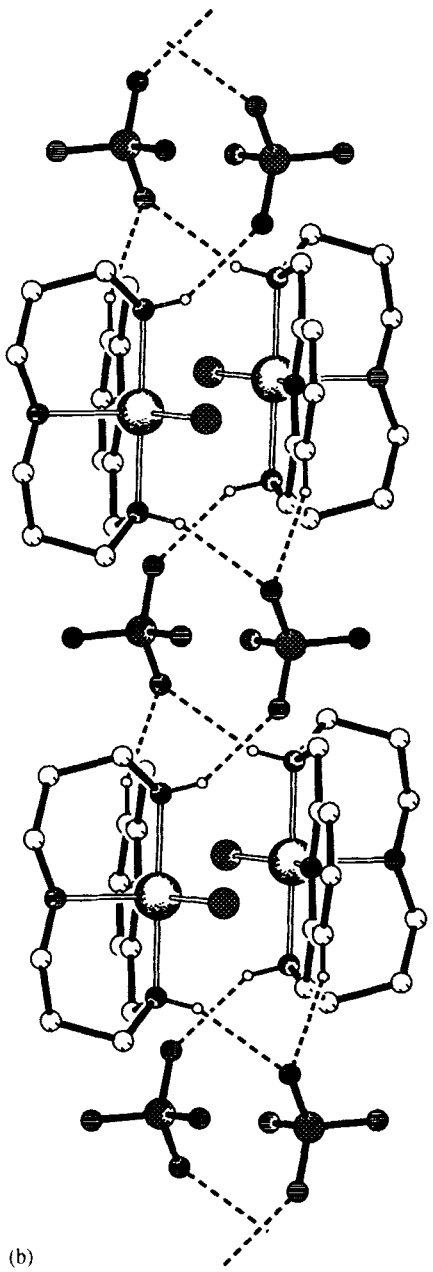

(b)

FIGURE 4 (Continued).

the 14-membered oxatriaza macrocyles L^2 and L^{12}, $[CuL^2(H_2O)]^{2+}$ **9** [2] and $[CuL^{12}Cl]^+$ **10** [2], in which the four donor atoms of the macrocycles define the equatorial co-ordination plane, display significantly shorter Cu–O equatorial distances of 2.031(8) and 1.998(5) Å, respectively. The Cu–Cl distance of 2.280(1) Å in **1** is within the expected value.

The **+−+e** conformation is also adopted by the macrocycle L^7 in the square-pyramidal nickel(II) complexes $[NiL^7(dmso)]^{2+}$ [32], $[NiL^7(Cl)]^+$ [32] and $[NiL^7(H_2O)]^{2+}$ [33] as well

Downloaded At: 15:31 29 January 2011

Downloaded At: 15:31 29 January 2011

as in the complex $[ZnL^9Cl]^+$ [31] in which the monodentate ligands, dmso, Cl, H_2O and Cl, respectively, complete the equatorial co-ordination sphere. By contrast the copper(II) complexes $[CuL^6(NO_3)]^+$ **3** [7], $[CuL^9I]^+$ **7** [31] and $[CuL^9Cl]^+$ **8** [31], quoted above, exhibit a planar conformation **−−−a**, in which the N-substituents are positioned below the N_4 equatorial co-ordination plane and opposite to the apical ligands, NO_3^-, I^- or Cl^-. The label **a** indicates that the monodentate ligand is in apical position.

This set of results indicate that the macrocycles L^1, L^3, L^6–L^9 adopt only two different forms, **+−+e** and **−−−a**, in five-coordinated transition metal complexes. It is also apparent that the replacement in L^3 of the nitrogen atom *trans* to the pyridine ring by an oxygen to give L^1 has not a significant influence on the structural preferences of the macrocycle. Unfortunately crystal structures of L^1 complexes having the **−−−a** arrangement do not exist [34]. Indeed to the best of our knowledge the complex $[CuL^1]^+$ **1** is the first metal complex of L^1 characterised by single crystal X-ray diffraction.

In the Figure 4 is shown the crystal-packing diagram of the complex **1** in two different views providing a clear picture of the structure of this compound in the solid state. The view along the *a* crystallographic axis presented in Figure 4a reveals chains of $[CuL^1Cl]^+$ cations intercalated by chains of ClO_4^- anions. In addition the molecular assembly of cations belonging to neighbour chains, related by a crystallographic inversion centre, results in a π-stacking of their pyridine rings in a cofacial geometric arrangement with an inter-planar distance between two adjacent aromatic rings of *ca.* 3.62 Å.

The analysis of the intermolecular contacts indicates that the crystal packing described above is stabilised by $C-H^{\delta+}\cdots O^{\delta-}$ and N–H···O hydrogen bonding interactions between the pyridine ring and the two NH groups of adjacent cations with oxygen atoms of ClO_4^- anions as shown in Figure 4b. Cations of the adjacent chains are connected by two oxygen atoms of ClO_4^- bridges *via* N–H···O hydrogen bonding leading to the formation of 1-*D* polymeric chain of cations and anions running along the *b* crystallographic axis. The two independent N–H···O intermolecular contacts found have O distances of 2.29(5) Å and N–H···O angles of 148(6) and 158(6)° respectively. Furthermore two adjacent chains of cations and anions related by a crystallographic inversion centre are linked by $C-H^{\delta+}\cdots O^{\delta-}$ short charge assisted interactions [C–H···O distances of 2.55 Å and angle of 161°] due to the involvement of an oxygen atom of ClO_4^- anions in a bifurcated arrangement with one NH group and one pyridine ring. Therefore the crystal presents a centrosymmetric supramolecular structure composed of cations and anions aggregated by hydrogen bonding interactions.

Finally the inter-planar distance between adjacent aromatic rings, quoted above, may represent simply the minimum *van der Waals* distance approach between these rings having not structural relevance. However, it is interesting to note that the inter-planar distance is precisely the distance between two pyridine rings of adjacent polymeric chains, connected by $C-H^{\delta+}\cdots O^{\delta-}$ and N–H···O hydrogen bonds.

Conclusions

This work has shown that the metal complexes of the 14-membered oxatriaza and tetraaza macrocycles, L^1 and L^3, display the same structural preferences. Both macrocycles have enough flexibility to adopt the **+−+e** folded conformation. This means that the replacement of the nitrogen *trans* to the pyridine ring of the 14-membered macrocycle L^3 by an oxygen to give L^1 has not a remarkable influence on the complexation behaviour. The differences of stability constants found for the corresponding metal complexes of both ligands are mainly due to electronic effects and consequently they are of the same magnitude as those found for similar

linear ligands, such as $H_2N(CH_2)_2O(CH_2)_2NH_2$ and $H_2N(CH_2)_2NH(CH_2)_2NH_2$ [5,35].

A detailed study of the conformational preferences of L^3 in five co-ordinated transition metal complexes was carried out by molecular mechanics calculations (MM) [7]. Values of the steric energy *versus* M–N distance calculated for this macrocycle with the metal ion in a five co-ordinated environment indicated that for distances M–N up to 2.15 Å there are three preferred conformations, having in common an axial monodentate ligand. The most stable conformation up to M–N distances of ≈1.90 Å is **+++a**, followed by **−−+a** between 1.90 and 2.05 Å and **−−−a** between 2.05 and 2.15 Å. The equatorial **+−+e** form is favoured for distances longer than 2.15 Å. Therefore, based in these results **+++a** or **−−+a** conformations will be expected for L^1. However these calculations were made considering a symmetrical co-ordination sphere and the complex **1** displays a strongly distorted one with a Cu–O distance of 2.247(4) Å longer than the Cu–N ones [2.002(5) Å]. So the apical elongation distortion favours the folded conformation **+−+e**. Moreover planar conformations, such as **+++a** and **−−+a**, would exist and will probably appear in future complexes involving this ligand.

Finally, the co-ordination behaviour of L^1 depends on a delicate balance between the electronic and geometric preferences of the transition metal ion and the steric constraints of the macrocyclic backbones.

EXPERIMENTAL

Reagents

All the chemicals were of reagent grade and used as supplied without further purification. The reference used for the ^1H NMR measurements in D_2O was 3-(trimethylsilyl)-propanoic acid-d_4-sodium salt and in $CDCl_3$ the solvent itself. For ^{13}C NMR spectra dioxane was used as internal reference.

Synthesis of 7-Oxa-3,11,17-triazabicyclo[11.3.1]heptadeca-1(17),13,15-triene (L^1)

An aqueous solution of $Cu(NO_3)_2 \cdot 3H_2O$ (3.7 mmol, 0.895 g, 10 cm^{-3}) was added to a solution of 2,6-pyridinedicarbaldehyde (3.7 mmol; 0.50 g, 8 cm^{-3}) in ethanol. To this stirred mixture was added dropwise a solution of bis(3-aminopropyl)ether (3.7 mmol; 0.489 g) in ethanol (2 cm^{-3}) over a period of 3.5 h. This blue-turquoise solution was refluxed for 4 h turning to dark blue. The copper(II) diimine complex formed was reduced by sodium borohydride (9.35 mmol; 0.355 g) added in small portions over a period of 30 min. at room temperature and then the mixture was warmed at 60°C for 30 m. The copper was removed by precipitation of its sulfide by addition of $Na_2S \cdot 9H_2O$ (8.5 mmol; 2.04 g). The filtrate was extracted with dichloromethane (4 × 20 cm^{-3}), the organic layer dried with $MgSO_4$ and then concentrated under vacuum. A yellow precipitate was obtained which was purified through a neutral alumina column (2.5 × 20 cm), using chloroform as eluent. Yield: 35%. m.p. 73–74°C. NMR ($CDCl_3$, TMS): δ 1.61 (4 H of $CH_2CH_2CH_2$, q), 2.37 (4 H of $NCH_2CH_2CH_2O$, t), 2.85 (2 H of N*H*, broad), 3.34 (4 H of $OCH_2CH_2CH_2N$, t), 3.67 (4 H of NCH_2Py, s), 6.80 (2 H of py in *m* position, d), 7.31 (1 H of py in *p* position, t). ^{13}C NMR ($CDCl_3$): δ 29.17 ($CH_2CH_2CH_2$), 44.79 ($NCH_2CH_2CH_2O$), 53.75 ($OCH_2CH_2CH_2N$), 67.76 (NCH_2Py), 120.28 (*m*-Cpy), 136.10 (*p*-Cpy) and 158.68 (*o*-Cpy). Found: C, 61.7; H, 9.1; N, 16.4%. Calc. for $C_{13}H_{21}N_3O \cdot H_2O$: C, 61.6; H, 9.2; N, 16.6%.

Caution although no problems were found in this work, perchlorates in presence of organic matter are potentially explosive and should be prepared in small quantities.

Downloaded At: 15:31 29 January 2011

Synthesis of the Complex $[CuL^1Cl](ClO_4)$, 1

An aqueous solution of $Cu(ClO_4)_2 \cdot 6H_2O$ (0.5 mmol, 0.185 g) was added to a stirred solution of $L^1 \cdot (HCl)_3$ (0.5 mmol, 0.173 g) dissolved in a minimum volume of water ($\approx 2\,cm^3$), the pH increased to about 5 with KOH and the mixture was stirred for 2 h. The precipitate formed was filtered off and dissolved in a mixture of ethanol/petroleum ether (40–60°C). Blue crystals were formed in thirty five days by slow evaporation of the solvent at room temperature. Yield: ≈85%.

Potentiometric Measurements

Reagents and Solutions

Metal ion solutions were prepared at about 0.025 mol dm^{-3} from the nitrate salts of the metals, of analytical grade with demineralized water (obtained by a Millipore/Milli-Q system) and were standardised as described [10, 29, 31]. Carbonate-free solutions of the titrant, KOH, were obtained, maintained and discarded as described [10, 29, 31].

Equipment and Work Conditions

The equipment used was described before [10, 29, 31]. The temperature was kept at 25.0 ± 0.1°C; atmospheric CO_2 was excluded from the cell during the titration by passing purified argon across the top of the experimental solution in the reaction cell. The ionic strength of the solutions was kept at 0.10 mol dm^{-3} with KNO_3, because we have verified that L^1 does not form complexes with K^+.

Measurements

The $[H^+]$ of the solutions was determined by the measurement of the electromotive force of the cell, $E = E'^{o} + Q\log[H^+] + E_j \cdot E'^{o}$, Q, E_j and $K_w = ([H^+][OH])$ were obtained as described previously [10, 29]. The term pH is defined as $-\log [H^+]$. The value of K_w was found equal to $10^{-13.80}\,mol^2dm^{-6}$.

The potentiometric equilibrium measurements were made on 20.00 cm^3 of $\cong 2.50 \times 10^{-3}$ mol dm^{-3} ligand solutions diluted to a final volume of 30.00 cm^3, in the absence of metal ions and in the presence of each metal ion for which the $C_M : C_L$ ratios were 1 : 1 and 1 : 2. A minimum of two replicates were made.

The equilibrium for the complex formation reactions was fast to attain. The same values of stability constants were obtained either using the direct or the back titration curves.

Calculation of Equilibrium Constants

Protonation constants $K_i^H = ([H_iL]/[H_{i-1}L][H])$ were calculated by fitting the potentiometric data obtained for the free ligand to the HYPERQUAD program [36]. Stability constants of the various species formed in solution were obtained from the experimental data corresponding to the titration of solutions of different metal ions to ligand ratios, also using the HYPERQUAD program. The initial computations were obtained in the form of overall stability constants, $\beta_{M_mH_hL_l}$ values, $\beta_{M_mH_hL_l} = ([M_mH_hL_l]/[M]^m[L]^l[H]^h)$.

Only mononuclear species, ML, MHL and M–HL (being $\beta_{M-HL} = \beta_{MLOH} \times K_w$) were found. Differences, in log units, between the values β_{MHL} (or β_{M-HL}) and β_{ML} provide the stepwise protonation reaction constants, shown in Table I. The errors quoted are the standard deviations of the overall stability constants given directly by the program for the input data which include all the experimental points of all titration curves. The standard deviations of the stepwise constants were determined by the normal propagation rules.

The protonation constants were obtained from 150 experimental points (3 titration curves) and

Downloaded At: 15:31 29 January 2011

the stability constants for each metal ion were determined from 100 to 150 experimental points (2 to 4 titration curves). All the points of a titration were used in the calculations except for those obtained with a simultaneous formation of a precipitate, which generally do not stabilise.

Spectroscopic Studies

^{1}H NMR spectra were recorded with a Bruker CXP-300 spectrometer at probe temperature. Magnetic moments of the complexes were determined by the Evans method in solution, at room temperature [37]. Electronic spectra were measured with a Shimadzu model UV-3100 spectrophotometer for UV-*vis*-near IR, using aqueous solutions of the complexes prepared by the addition of the metal ion (in the form of nitrate salt) to the ligand at the appropriate pH value. EPR spectroscopy measurements of the Cu^{2+} complexes were recorded with a Bruker ESP 380 spectrometer equipped with continuous-flow cryostats for liquid nitrogen, operating at X-band. The complex was prepared in 1.25×10^{-3} mol dm^{-3} in 1.0 mol dm^{-3} $NaClO_4$ at pH values between 3.90 and 6.10 and were recorded at 127 K.

Crystallography

Suitable single crystals of $[CuL^1Cl](ClO_4)$ **1** for X-ray diffraction studies were grown from an aqueous solution at room temperature. X-ray data were collected at room temperature using a MACH3, with graphite monochromated Mo-K_α radiation ($\lambda = 0.71069$ Å) using a ω-2θ scan mode. Unit cell dimensions for complex **1** were obtained by least-squares refinement of the setting angles of 25 reflections with θ between 18 and 25°. Data were corrected for Lorentz, polarisation and linear decay (no decay was observed) as well as empirically for absorption, using the MOLEN software [38].

Crystal Data

$C_{13}H_{21}CuN_3O_5Cl_2$, M 433.77, triclinic, space group $P\bar{1}$, $a = 7.4973(9)$, $b = 9.649(2)$, $c = 12.712(2)$ Å, $\alpha = 111.02(2)$, $\beta = 96.65(1)$, $\gamma = 90.11(1)°$, $V = 851.7(2)$ Å^3, $Z = 2$, $D_{calcd} = 1.691$ g cm^{-3}, $F(000) = 446$, $\mu = 1.625$ mm^{-1}.

Intensities of 3550 reflections were measured of which 3339 were unique reflections giving a R_{int} of 0.0118. The structure was solved by a combination of direct methods and Fourier difference syntheses and refined by least squares on F^2. All non-hydrogen atoms were refined with anisotropic thermal parameters. All hydrogen atoms were inserted in idealised positions and allowed to refine, riding in the parent carbon atom with an isotropic thermal parameter equal to 1.2 times those to which they were bonded. Exceptions were the hydrogen atoms bonded to the nitrogen atoms N(1) and N(7), which were located in the Fourier difference maps and allowed to refine with individual isotropic thermal parameters with the N–H distances constrained to 0.86 Å.

Large anisotropic thermal displacements were obtained for the oxygen atoms of counter ion ClO_4^-, suggesting that this anion was affected by some thermal or/and positional disorder. Many trial refinements were performed using different disorder models for ClO_4^- anion. However no trial models tested gave satisfactory results either in terms of a reasonable overall geometry for the anion or a pronounced decrease of the R values. Therefore in final refinements the thermal movement of the oxygen atoms of the ClO_4^- anion were described with anisotropic parameters.

The final refinement of 215 parameters converged to R and R' of 0.0578 and 0.1454 for 2603 reflections with $I > 2\sigma(I)$ and 0.0782 and 0.1619 for all data. A final GOF (goodness-of-fit) of 1.088 was obtained. The final Fourier difference synthesis revealed residual electron densities of 1.332, -0.509 eÅ^{-3}. The positive peak was

Downloaded At: 15:31 29 January 2011

within 0.39 Å of the chlorine bonded to the copper centre.

All calculations to solve and refine the structures were carried out with SHELXS and SHELXL from the SHELX97 package [39]. Molecular and Crystal packing diagrams were drawn with PLATON [40] and WEBLAB VIEWER [41] graphical software packages.

Acknowledgements

The authors acknowledge the financial support of FCT and PRAXIS XXI (Project n. PRAXIS/2/2.1/QUI/17/94).

References

[1] Amorim, M. T. S., Chaves, S., Delgado, R. and Fraústo da Silva, J. J. R. (1991). *J. Chem. Soc., Dalton Trans.*, p. 3065.
[2] Félix, V., Delgado, R., Amorim, M. T. S., Chaves, S., Galvão, A. M., Duarte, M. T., Carrondo, M. A. A. F. C. T., Moura, I. and Fraústo da Silva, J. J. R. (1994). *J. Chem. Soc., Dalton Trans.*, p. 3099.
[3] Hancock, R. D. (1992). *J. Chem. Educ.*, **69**, 615.
[4] Martell, A. E., Hancock, R. D. and Motekaitis, R. J. (1994). *Coord. Chem. Rev.*, **133**, 39.
[5] Cabral, M. F., Costa, J., Delgado, R., Fraústo da Silva, J. J. R. and Vilhena, M. F. (1990). *Polyhedron*, **9**, 2847.
[6] Costa, J. and Delgado, R. (1993). *Inorg. Chem.*, **32**, 5257.
[7] Félix, V., Calhorda, M. J., Costa, J., Delgado, R., Brito, C., Duarte, M. T., Arcos, T. and Drew, M. G. B. (1996). *J. Chem. Soc., Dalton Trans.*, p. 4543.
[8] Balakrishnan, K. P., Omar, H. A. A., Moore, P., Alcock, N. W. and Pike, G. A. (1990). *J. Chem. Soc., Dalton Trans.*, p. 2965.
[9] Hancock, R. D. and Martell, A. E. (1989). *Chem. Rev.*, **89**, 1875.
[10] Cabral, M. F., Delgado, R., Duarte, M. T. and Teixeira, M. (2000). *Helv. Chim. Acta*, **83**, 702.
[11] Bertini, I. and Luchinat, C. (1984). *Adv. Inorg. Biochem.*, **6**, 71.
[12] Lever, A. B. P., *Inorganic Electronic Spectroscopy*, 2nd edn., Elsevier, Amsterdam, 1984.
[13] Sacconi, L., Mani, F. and Bencini, A. (1987). In: *Comprehensive Coordination Chemistry*, Wilkinson, G., Gillard, R. D. and McCleverty, J. A. (Eds.), Pergamon Press, **V**, 1–137.
[14] Ciampolini, M. and Nardi, N. (1966). *Inorg. Chem.*, **5**, 41; *ibid., Inorg. Chem.* (1967). **6**, 445.
[15] Ciampolini, M. (1966). *Inorg. Chem.*, **5**, 35.
[16] Renfrew, R. W., Jamison, R. S. and Weatherburn, D. C. (1979). *Inorg. Chem.*, **18**, 1584.
[17] Chaves, S., Cerva, A. and Delgado, R. (1997). *J. Chem. Soc., Dalton Trans.*, p. 4181.
[18] Smierciak, R., Passariello, J. and Blinn, E. L. (1977). *Inorg. Chem.*, **16**, 2646.
[19] Neese, F., *Diploma Thesis*, University of Konstanz (Germany), June, 1993.
[20] Li, Y. (1996). *Bull. Chem. Soc. Jpn.*, **69**, 2513.
[21] Hathaway, B. J. (1983). *Coord. Chem. Rev.*, **52**, 87.
[22] Yokoi, H., Sai, M., Isobe, T. and Ohsawa, S. (1972). *Bull. Chem. Soc. Jpn.*, **45**, 2189.
[23] Lau, P. W. and Lin, W. C. (1975). *J. Inorg. Nucl. Chem.*, **37**, 2389.
[24] Costa, J., Delgado, R., Figueira, M. C., Henriques, R. T. and Teixeira, M. (1997). *J. Chem. Soc., Dalton Trans.*, p. 65.
[25] Styka, M. C., Smierciak, R. C., Blinn, E. L., DeSimone, R. E. and Passariello, J. V. (1978). *Inorg. Chem.*, **17**, 82.
[26] Miyoshi, K., Tanaka, H., Kimura, E., Tsuboyama, S., Murata, S., Shimizu, H. and Ishizu, K. (1983). *Inorg. Chim. Acta*, **78**, 23.
[27] Reinen, D., Ozarowski, A., Jakob, B., Pebler, J., Stratemeier, H., Wieghardt, K. and Tolksdorf, I. (1987). *Inorg. Chem.*, **26**, 4010.
[28] Chaudhuri, P., Oder, K., Wieghardt, K., Weiss, J., Reedijk, J., Hinrichs, W., Wood, J., Ozarowski, A., Stratemaier, H. and Reinen, D. (1986). *Inorg. Chem.*, **25**, 2951.
[29] Costa, J., Delgado, R., Drew, M. G. B. and Félix, V. (1999). *J. Chem. Soc., Dalton Trans.*, p. 4331.
[30] Lu, T.-H., Tung, S.-F., Chi, T.-Y. and Chung, C.-S. (1998). *Acta Cryst.*, **C54**, 1069.
[31] Costa, J., Delgado, R., Drew, M. G. B., Félix, V. and Saint-Maurice, A. (2000). *J. Chem. Soc., Dalton Trans*, p. 1907.
[32] Alcock, N. W., Moore, P. and Omar, H. A. A. (1987). *J. Chem. Soc., Dalton Trans.*, p. 1107.
[33] Foster, K. A., Barefield, E. K. and van Derver, G. (1986). *J. Chem. Soc., Dalton Trans.*, p. 680.
[34] Allen, F. H., Davies, J. E., Galloy, J. J., Johnson, O., Kennard, O., Macrae, C. F. and Watson, D. G. (1991). *J. Chem. Inf. Comp. Sci.*, **31**, 204.
[35] (a) Smith, R. M., Martell, A. E. and Motekaitis, R. J., *Nist Critical Stability Constants of Metal Complexes Database*, U.S. Department of Commerce, Gaithersburg, 1993; (b) Pettit, L. D. and Powell, H. K. J., *IUPAC Stability Constants Database*, Academic Software, Timble, 1993.
[36] Gans, P., Sabatini, A. and Vacca, A. (1996). *Talanta*, **43**, 1739.
[37] Evans, D. F. (1959). *Chem. Soc.*, p. 2003.
[38] Enraf Nonius, "MOLEN Data reduction software".
[39] Sheldrick, G. M., *SHELX-97*, University of Göttingen, 1997.
[40] Spek, A. L., *PLATON, a Multipurpose Crystallographic Tool*, Utrecht University, Utrecht, The Netherlands, 1999.
[41] WEBLAB VIEWER, *version 2.01*, Molecular Simulations, Inc., San Diego, 1997.

Downloaded At: 15:31 29 January 2011